Vol. 7, No. 4, August 2023, pp. 449-456

Current Optics and Photonics

Regular Paper

Theoretical Results for a Dipole Plasmonic Mode Based on a Forced Damped Harmonic Oscillator Model

Tongtong Hao and Quanshui Li*

Department of Applied Physics, School of Mathematics and Physics, University of Science and Technology Beijing, Beijing 100083, China

(Received February 7, 2023 : revised May 26, 2023 : accepted May 31, 2023)

The localized surface-plasmon resonance has drawn great attention, due to its unique optical properties. In this work a general theoretical description of the dipole mode is proposed, using the forced damped harmonic oscillator model of free charges in an ellipsoid. The restoring force and driving force are derived in the quasistatic approximation under general conditions. In this model, metal is regarded as composed of free charges and bound charges. The bound charges form the dielectric background which has a dielectric function. Those free charges undergo a collective motion in the dielectric background under the driving force. The response of free charges will not be included in the dielectric function like the Drude model. The extinction and scattering cross sections as well as the damping coefficient from our model are verified to be consistent with those based on the Drude model. We introduce size effects and modify the restoring and driving forces by adding the dynamic depolarization factor and the radiation damping term to the depolarization factor. This model provides an intuitive physical picture as well as a simple theoretical description of the dipole mode of the localized surface-plasmon resonance based on free-charge collective motion.

Keywords : Dipole mode, Forced damped harmonic oscillator model, Free charges, Localized surface plasmon resonance (LSPR), Resonance frequencies

OCIS codes : (160.4236) Nanomaterials; (230.4910) Oscillators; (240.6680) Surface plasmons; (250.5403) Plasmonics

I. INTRODUCTION

Metallic nanostructures have attracted widespread attention for their fantastic optical properties, due to the abundant free electrons in metals. When these electrons are constrained within a limited volume, their collective motion (which is driven by the external light field and modulated by bound charges at the interface of the metal and the medium) generates the localized surface-plasmon resonance (LSPR) [1]. The LSPR of metallic nanoparticles exhibits intense absorption and scattering cross-sections in the far field. It can generate large local electric field enhancement in some regions [2, 3], and a local heat source from the plasmonic nanoparticles [3, 4]. The resonance wavelengths can be tuned by size and shape of the plasmonic nanoparticles, while recently doped semiconductors have attracted extra attention for tunable resonances due to their variable carrier density [3, 5–9]. The LSPR has applications in a wide range of fields, including biosensors [7, 10–12], solar cells [8, 12, 13], nanoantennae [14], and therapeutic applications [3, 4, 6, 15–17].

The LSPR is the interaction of the incident light with metal nanoparticles, which can be described by Maxwell's equations and the dielectric function of the metal (in the Drude model). For quantitative research, numerical simulations are performed using many algorithms, such as the

*Corresponding author: qsli@ustb.edu.cn, ORCID 0000-0002-4908-9160

Color versions of one or more of the figures in this paper are available online.

This is an Open Access article distributed under the terms of the Creative Commons Attribution Non-Commercial License (http://creativecommons.org/licenses/by-nc/4.0/) which permits unrestricted non-commercial use, distribution, and reproduction in any medium, provided the original work is properly cited.

Copyright © 2023 Current Optics and Photonics

pISSN: 2508-7266 / eISSN: 2508-7274 https://doi.org/10.3807/COPP.2023.7.4.449

finite-difference time-domain (FDTD) and discrete-dipole approximation (DDA), for arbitrary shapes of particles. Mie theory [18] provides a rigorous solution for spherical nanoparticles. A typical way in textbooks to analyze the LSPR is by considering a dielectric sphere with the dielectric function of the metal under a uniform external field, in a quasistatic approach [18]. For the electric dipole mode, the resonance condition (Fröhlich condition) can be derived from one coefficient of Mie theory, or the quasistatic approach with the dielectric function of the Drude model [18]. As we all know, the Drude model arises from the collective motion of free charges in metals, so the LSPR in Mie theory and the quasistatic approximation is associated with the collective motion of free charges through the dielectric function of the metal. Additionally, the hydrodynamic model [19] and the hybridization model [20] are also used to describe the LSPR based on the collective motion of free electrons, but those models are not as intuitive as the forced damped harmonic oscillator model. A more intuitive physical picture is that free charges oscillate within the domain of a nanoparticle under the electric field of the incident light. The harmonic oscillator model is reasonable for this collective motion. This model can explain many phenomena, including damping [21], coupling [22], and resonance frequencies in the near field and far field [23, 24]. There is no thorough theoretical derivation for the LSPR based on this model, except for our previous work [1]. In that work, the metal is divided into free charges and the dielectric background, which has a dielectric function. Free charges generate the collective motion under the electric field, and the influence of free charges does not appear in the dielectric function. We have derived the theoretical description for the dipole mode of an ellipsoidal nanoparticle under the special condition that there is a $\pi/2$ phase difference between the displacement and the external field at the resonance frequency. Nevertheless, this is not a general theoretical description, for some important information is not contained in it due to this special condition. Moreover, size effects are also not included in the previous results. According to the modified long-wavelength approximation, the dynamic depolarization factor and radiation damping term can be introduced into the forced damped harmonic oscillator model [25, 26].

In this paper, we first derive a theoretical description based on a subwavelength ellipsoid under general conditions. The restoring force, driving force, and extinction and scattering cross sections of the LSPR and its resonance frequencies, are obtained using the forced damped harmonic oscillator model. We then compare the results, including the extinction and scattering cross sections, from our model to those from the dielectric function of the Drude model. To account for the size effects, we introduce the dynamic depolarization factor and radiation damping term into the harmonic oscillator model. Finally, we discuss some conclusions from the harmonic oscillator model.

II. THEORETICAL MODEL

The relative dielectric function of the metal $\varepsilon(\omega)$ always includes a contribution from free charges, which is described by the Drude model. $\varepsilon(\omega)$ is usually described as follows [27]:

$$\varepsilon(\omega) = \varepsilon_\infty - \frac{\omega_p^2}{\omega^2 + \gamma^2} + i\frac{\omega_p^2 \gamma}{\omega^3 + \gamma^2 \omega}, \tag{1}$$

where ω_p is the plasma frequency and γ is the damping coefficient. The first term ε_∞ is the high-frequency dielectric function arising from the bound charges of the lattice, and the second and third terms arise from the Drude model based on free charges.

In our model, the metal is divided into two parts: The dielectric background, and free charges. Free charges include free electrons (negative) and the related lattice background (positive), with equal charge densities. In other words, the metal is regarded as a dielectric that contains equal negative and positive free charges. The bound charges of the dielectric background generate the relative dielectric function ε_∞. The response of free charges to light is considered as a collective motion driven by an external field, rather than included in the dielectric function of the metal. The approach in which the metal is divided into two parts is similar to that of the Huang equations, in which the ionic crystal is divided into two parts: the positive and negative ions, and the bound charges of those ions [28].

When the particle size, such as the radius a, is much smaller than the wavelength λ of light, for example $a < \lambda/20$ [29], the particle is regarded to be in a uniform external field, which is the quasistatic approximation (the electrostatic approach) [18]. To obtain analytical results, the particle is usually assumed to be a sphere to derive the fundamental conclusions. Sometimes it is assumed to be an ellipsoid, to include the shape effects. On the other hand, many practical nanoparticles can be approximated as ellipsoids.

A dielectric ellipsoid containing free charges with relative dielectric function ε_∞ is located in a medium with relative dielectric function ε_m under a uniform external electric field E_0, as shown in Fig. 1. The magnitude of the charge density of the positive and negative free charges in this ellipsoid is set as ρ. Two ellipsoids formed by the positive and negative free charges separate from each other under the external field, and the distance between the centers of the two ellipsoids is set as d, which can be regarded as the displacement of the oscillator formed by free charges. a and b are the principal semiaxes of the ellipsoid.

When the light irradiates this ellipsoid, free charges accumulate on its surface and generate an additional electric field. The electric field in the ellipsoid includes the external electric field, the additional electric field from the accumulated surface free charges, and that from the surface bound charges from the lattice and the surrounding me-

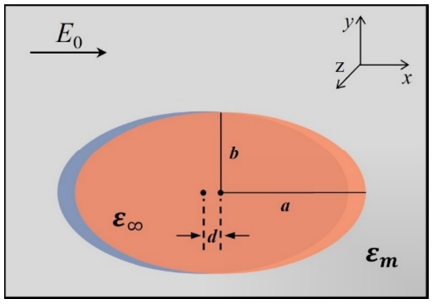

FIG. 1. Schematic diagram of the forced damped harmonic oscillator model. In this model, free charges in a dielectric ellipsoid with relative dielectric function ε_∞ are divided into two ellipsoids of equal and opposite charge density under the external field E_0. The distance between the centers of the two ellipsoids is d. The relative dielectric function of the medium is ε_m. a and b are the principal semiaxes of the ellipsoid.

dium. The collective motion of free charges driven by the external field in a nanoparticle should be a forced motion with damping effects, so it is reasonable to use the forced damped harmonic oscillator model to describe the LSPR.

In the electrostatic approach, the potential in space satisfies the Laplace equation, $\nabla^2\varphi_1 = 0$ and $\nabla^2\varphi_2 = 0$, where φ_1 and φ_2 are the potential inside and outside the ellipsoid respectively. The potential is solved in ellipsoidal coordinates [30, 31]. The relationship between ellipsoidal coordinates and Cartesian coordinates is

$$\frac{x^2}{a^2+u}+\frac{y^2}{b^2+u}+\frac{z^2}{c^2+u}=1, \tag{2}$$

where a, b, and c are the principal semiaxes of the ellipsoid. This equation has three different real roots: ξ, η, and ζ.

The potential of a uniform external field E_0 along the x axis is written as

$$\varphi_0 = -E_0 x = \mp E_0 \frac{\sqrt{(\xi+a^2)(\eta+a^2)(\varsigma+a^2)}}{\sqrt{(b^2-a^2)(c^2-a^2)}}. \tag{3}$$

The potential inside and outside the ellipsoid can be written as

$$\varphi_1 = \varphi_1' = C_1\varphi_0, \tag{4}$$

$$\varphi_2 = \varphi_0 + \varphi_2' = \left(1 + C_2\int_\xi^\infty \frac{ds}{R_s(s+a^2)}\right)\varphi_0, \tag{5}$$

where φ_1' is from the surface charges of the ellipsoid. φ_2' is set as

$$\varphi_2' = \varphi_0 F(\xi). \tag{6}$$

The expression for $F(\xi)$ is

$$F(\xi) = C_2\int_\xi^\infty \frac{ds}{R_s(s+a^2)}, \tag{7}$$

where $R_s = \sqrt{(s+a^2)(s+b^2)(s+c^2)}$.

The Laplace equation including $F(\xi)$ is

$$\frac{d^2F}{d\xi^2}+\frac{dF}{d\xi}\frac{d}{d\xi}\ln[R_\xi(\xi+a^2)]=0. \tag{8}$$

According to the boundary conditions ($\xi = 0$),

$$\varphi_{1,H} = \varphi_{2,H}, \tag{9}$$

$$-\varepsilon_m\varepsilon_0\frac{\partial\varphi_{2,H}}{\partial n}+\varepsilon_\infty\varepsilon_0\frac{\partial\varphi_{1,H}}{\partial n} = \sigma_f, \tag{10}$$

where σ_f is the surface free-charge density function that we set. $\varphi_{1,H}$ and $\varphi_{2,H}$ are the potential inside and outside the ellipsoid in our harmonic oscillator model respectively. The subscript H indicates the harmonic model. The normal derivative of the potential in ellipsoidal coordinates is

$$\frac{\partial\varphi}{\partial n} = \frac{\partial\varphi}{h_1\partial\xi}, \tag{11}$$

where $h_1 = \sqrt{(\xi-\eta)(\xi-\zeta)}\,/\,2R_\xi$.

If there are no free charges, or the response of free charges is attributed to the dielectric function as in the Drude model, the boundary conditions are

$$\varphi_{1,D} = \varphi_{2,D}, \tag{12}$$

$$-\varepsilon_m\varepsilon_0\frac{\partial\varphi_{2,D}}{\partial n}+\varepsilon\varepsilon_0\frac{\partial\varphi_{1,D}}{\partial n} = 0, \tag{13}$$

where the subscript D indicates the Drude model. Those are the usual boundary situations for an ellipsoid with the relative dielectric function $\varepsilon(\omega)$. Here we give the well-known results in textbooks [18], to compare to our results later. The potential inside and outside the ellipsoids with the Drude model are obtained as follows:

$$\varphi_{1,D} = \frac{\varepsilon_m}{\varepsilon_m+(\varepsilon-\varepsilon_m)n^{(x)}}\varphi_0, \tag{14}$$

$$\varphi_{2,D} = \left[1-\frac{1}{2}\frac{abc(\varepsilon-\varepsilon_m)}{\varepsilon_m+(\varepsilon-\varepsilon_m)n^{(x)}}\int_\xi^\infty\frac{ds}{R_s(s+a^2)}\right]\varphi_0, \tag{15}$$

where $n^{(x)}$ is the depolarization factor along the x direction, which is closely associated with the shape. The depolarization factor is

$$n^{(x)} = \frac{abc}{2}\int_0^\infty\frac{ds}{R_s(s+a^2)}. \tag{16}$$

Considering a point far away from the ellipsoid, the distance between them is defined as r. When $r \to \infty$, $\xi \to \infty$ in the ellipsoidal coordinates, and then $\xi \approx r^2$ [31].

$$\int_{\xi}^{\infty}\frac{ds}{R_s(s+a^2)}=\int_{r^2}^{\infty}\frac{ds}{s^{5/2}}=\frac{2}{3r^3}. \tag{17}$$

So, the potential $\varphi_2'(r)$ is

$$\varphi_2'(r)=\frac{E_0 x}{r^3}\frac{V}{4\pi}\frac{\varepsilon-\varepsilon_m}{(\varepsilon-\varepsilon_m)n^{(x)}+\varepsilon_m}, \tag{18}$$

where $V = 4\pi abc/3$ is the volume of the ellipsoid. The potential is expressed in terms of the dipole moment as $\varphi_2'(r) = p/4\pi\varepsilon_0\varepsilon_m r^2$. Thus, the dipole moment p_D of the ellipsoid with the Drude model can be obtained:

$$p_D=\frac{4}{3}\pi abc\varepsilon_0\varepsilon_m\frac{\varepsilon-\varepsilon_m}{\varepsilon_m+(\varepsilon-\varepsilon_m)n^{(x)}}E_0. \tag{19}$$

Then, according to $p = \varepsilon_0\varepsilon_m\alpha E_0$, the polarizability α_D is

$$\alpha_D=\frac{4}{3}\pi abc\frac{\varepsilon-\varepsilon_m}{\varepsilon_m+(\varepsilon-\varepsilon_m)n^{(x)}}. \tag{20}$$

The extinction and scattering cross sections based on the Drude model are expressed as follows:

$$\begin{aligned}C_{ext,D}&=k\,\mathrm{Im}[\alpha]\\&=\frac{4}{3}\pi abck\,\mathrm{Im}\left[\frac{\varepsilon-\varepsilon_m}{\varepsilon_m+(\varepsilon-\varepsilon_m)n^{(x)}}\right],\end{aligned} \tag{21}$$

$$\begin{aligned}C_{sca,D}&=\frac{k^4}{6\pi}|\alpha|^2\\&=\frac{8}{27}\pi k^4a^2b^2c^2\left|\frac{\varepsilon-\varepsilon_m}{\varepsilon_m+(\varepsilon-\varepsilon_m)n^{(x)}}\right|^2,\end{aligned} \tag{22}$$

where k is the wave vector.

If the scattering is small compared to the absorption, $C_{ext,D}$ can be replaced by $C_{abs,D}$ in Eq. (21) [18].

III. RESULTS AND DISCUSSION

3.1. General Theoretical Results for the Harmonic Oscillator Model

Following Eqs. (9) and (10), we obtain the coefficients C_1 and C_2 as follows:

$$C_1=\frac{\varepsilon_m+2a^2h_1n^{(x)}\sigma_f/\varepsilon_0\varphi_0}{(\varepsilon_\infty-\varepsilon_m)n^{(x)}+\varepsilon_m}, \tag{23}$$

$$C_2=\frac{a^3bch_1\sigma_f/\varepsilon_0\varphi_0-abc(\varepsilon_\infty-\varepsilon_m)/2}{(\varepsilon_\infty-\varepsilon_m)n^{(x)}+\varepsilon_m}. \tag{24}$$

The potential inside ($\varphi_{1,H}$) and outside ($\varphi_{2,H}$) the ellipsoids can be written as follows:

$$\varphi_{1,H}=\frac{\varepsilon_m}{(\varepsilon_\infty-\varepsilon_m)n^{(x)}+\varepsilon_m}\varphi_0+\frac{2a^2h_1n^{(x)}\sigma_f/\varepsilon_0}{(\varepsilon_\infty-\varepsilon_m)n^{(x)}+\varepsilon_m}, \tag{25}$$

$$\begin{aligned}\varphi_{2,H}=\varphi_0+&\\&\frac{a^3bch_1\sigma_f/\varepsilon_0\varphi_0-abc(\varepsilon_\infty-\varepsilon_m)/2}{(\varepsilon_\infty-\varepsilon_m)n^{(x)}+\varepsilon_m}\\&\cdot\varphi_0\int_{\xi}^{\infty}\frac{ds}{R_s(s+a^2)}.\end{aligned} \tag{26}$$

The total surface charge density σ_{total}, including free charges and bound charges, is

$$\begin{aligned}\sigma_{\text{total}}&=-\varepsilon_0\left(\frac{\partial\varphi_2}{\partial n}-\frac{\partial\varphi_1}{\partial n}\right)\\&=\frac{1}{(\varepsilon_\infty-\varepsilon_m)n^{(x)}+\varepsilon_m}\sigma_f\\&\quad-\frac{\varphi_0}{2a^2h_1}(\varepsilon_\infty-\varepsilon_m)\frac{\varepsilon_0}{(\varepsilon_\infty-\varepsilon_m)n^{(x)}+\varepsilon_m}.\end{aligned} \tag{27}$$

The electric field generated by free charges in an ellipsoid is $E_f = \rho d n^{(x)}/\varepsilon_0$ [1], where d is displacement between the centers of the two ellipsoids formed by the positive and negative free charges.

The total electric field from free charges and bound charges in the ellipsoid is

$$\begin{aligned}E_{\text{total}}&=\frac{\sigma_{\text{total}}}{\sigma_f}E_f\\&=\frac{\varepsilon_\infty-\varepsilon_m}{\varepsilon_m+(\varepsilon_\infty-\varepsilon_m)n^{(x)}}E_0n^{(x)}+\frac{\rho d/\varepsilon_0}{\varepsilon_m+(\varepsilon_\infty-\varepsilon_m)n^{(x)}}n^{(x)},\end{aligned} \tag{28}$$

where the surface free-charge density σ_f is expressed as $\sigma_f = \rho x d/2a^2h_1$ [1]. The first term is related to the driving force, for it is associated with the external field. The second term is related to the restoring force, for it is proportionate to the displacement d. Then the equation of motion is

$$m\ddot{d}+m\gamma\dot{d}=e\left(E_0-E_{\text{total}}\right). \tag{29}$$

It can further be expressed as follows:

$$m\ddot{d}+m\gamma\dot{d}+m\omega_0^2d=eE_0\frac{\varepsilon_m}{\left(\varepsilon_\infty-\varepsilon_m\right)n^{(x)}+\varepsilon_m}, \tag{30}$$

where the restoring force is

$$F=-m\omega_0^2d=-m\frac{1}{\varepsilon_\infty-\varepsilon_m+\varepsilon_m/n^{(x)}}\omega_p^2d, \tag{31}$$

where $\omega_p^2 = \rho e/\varepsilon_0 m$; The constants e, m, and ε_0 are the elementary charge, the free electron's mass, and the vacuum permittivity respectively.

The actual driving force in Eq. (30) does not equal the force of the incident light field; it is weakened by the di-

electric functions of the medium and dielectric background.

The resonance frequency is

$$\omega_R = \sqrt{\omega_0^2 - \frac{\gamma^2}{2}}. \tag{32}$$

Because the damping coefficient γ is practically much smaller than ω_0, the above equation can be approximated as follows:

$$\omega_R \approx \omega_0 = \sqrt{\frac{1}{\varepsilon_\infty - \varepsilon_m + \varepsilon_m / n^{(x)}}}\omega_p. \tag{33}$$

From Eq. (30), the displacement d can be obtained as follows:

$$\begin{aligned} d &= \frac{eE_0}{m}\frac{\varepsilon_m}{(\varepsilon-\varepsilon_m)n^{(x)}+\varepsilon_m}\frac{1}{\omega_0^2-\omega^2-i\omega\gamma}\exp(-i\omega t) \\ &= AE_0\exp(i\varphi)\exp(-i\omega t), \end{aligned} \tag{34}$$

where

$$A = \frac{e}{m}\frac{\varepsilon_m}{(\varepsilon_\infty-\varepsilon_m)n^{(x)}+\varepsilon_m}\frac{1}{\sqrt{(\omega_0^2-\omega^2)^2+(\omega\gamma)^2}}, \tag{35}$$

$$\exp(i\varphi) = \frac{\omega_0^2-\omega^2+i\omega\gamma}{\sqrt{(\omega_0^2-\omega^2)^2+(\omega\gamma)^2}}. \tag{36}$$

Following Eqs. (17)–(19), the dipole moment of the ellipsoid is expressed as follows:

$$\begin{aligned} p_H &= \frac{4}{3}\pi abc\varepsilon_0\varepsilon_m\frac{1}{(\varepsilon_\infty-\varepsilon_m)n^{(x)}+\varepsilon_m}E_0 \\ &\cdot[\rho Ae^{i\varphi}/\varepsilon_0+(\varepsilon-\varepsilon_m)]. \end{aligned} \tag{37}$$

The polarization of the metal arises from the dipole moment formed by the positive and negative free charges and the polarization of the bound charges in the dielectric background.

The polarizability is

$$\alpha_H = \frac{4}{3}\pi abc\frac{1}{(\varepsilon_\infty-\varepsilon_m)n^{(x)}+\varepsilon_m}[\rho Ae^{i\varphi}/\varepsilon_0+(\varepsilon_\infty-\varepsilon_m)]. \tag{38}$$

The extinction and scattering cross sections can be expressed as follows:

$$\begin{aligned} C_{ext,H} &= k\,\mathrm{Im}[\alpha] \\ &= \frac{4}{3}\pi kabc \\ &\cdot\mathrm{Im}\left[\frac{\varepsilon_\infty-\varepsilon_m}{(\varepsilon_\infty-\varepsilon_m)n^{(x)}+\varepsilon_m}+\frac{\rho Ae^{i\varphi}/\varepsilon_0}{(\varepsilon_\infty-\varepsilon_m)n^{(x)}+\varepsilon_m}\right], \end{aligned} \tag{39}$$

$$\begin{aligned} C_{sca,H} &= \frac{k^4}{6\pi}|\alpha|^2 \\ &= \frac{8}{27}\pi k^4a^2b^2c^2 \\ &\cdot\left|\frac{\varepsilon_\infty-\varepsilon_m}{(\varepsilon_\infty-\varepsilon_m)n^{(x)}+\varepsilon_m}+\frac{\rho Ae^{i\varphi}/\varepsilon_0}{(\varepsilon_\infty-\varepsilon_m)n^{(x)}+\varepsilon_m}\right|^2. \end{aligned} \tag{40}$$

The extinction and scattering cross sections obtained from the two models (harmonic oscillator model and Drude model) are equivalent. The extinction cross section can be written as follows:

$$\begin{aligned} C_{ext,D} &= C_{ext,H} \\ &= \frac{4}{3}\pi kabc\frac{\varepsilon_m}{[(\varepsilon_\infty-\varepsilon_m)n^{(x)}+\varepsilon_m]^2}\omega_p^2 \\ &\cdot\frac{\omega\gamma}{(\omega_0^2-\omega^2)^2+(\omega\gamma)^2}, \end{aligned} \tag{41}$$

where ρ is converted to ω_p.

In the same way, the scattering cross section can be written as follows:

$$\begin{aligned} C_{sca,D} &= C_{sca,H} \\ &= \frac{8}{27}\pi k^4a^2b^2c^2\left(\frac{1}{(\varepsilon_\infty-\varepsilon_m)n^{(x)}+\varepsilon_m}\right)^2 \\ &\cdot[(\varepsilon_\infty-\varepsilon_m)^2 \\ &+\frac{2\varepsilon_m(\varepsilon_\infty-\varepsilon_m)}{(\varepsilon_\infty-\varepsilon_m)n^x+\varepsilon_m}\frac{\omega_p^2(\omega_0^2-\omega^2)}{(\omega_0^2-\omega^2)^2+(\omega\gamma)^2} \\ &+\left(\frac{\varepsilon_m}{(\varepsilon_\infty-\varepsilon_m)n^{(x)}+\varepsilon_m}\right)^2\frac{\omega_p^4}{(\omega_0^2-\omega^2)^2+(\omega\gamma)^2}]. \end{aligned} \tag{42}$$

According to the extinction and scattering cross sections obtained above, their resonance frequencies can be obtained as follows:

$$\omega_{ext}^2 = \omega_0^2, \tag{43}$$

$$\begin{aligned} \omega_{sca}^2 &\approx \omega_0^2 - \frac{[2(\varepsilon_\infty-\varepsilon_m)n^{(x)}-\varepsilon_m]\gamma^2}{2\varepsilon_m} \\ &-\frac{(\varepsilon_\infty-\varepsilon_m+9\varepsilon_\infty n^{(x)})n^{(x)}\gamma^4}{3\varepsilon_m\omega_0^2} \\ &+\frac{(\varepsilon_m^2+\varepsilon_\infty^2+\varepsilon_\infty\varepsilon_m)n^{(x)2}\gamma^4}{\varepsilon_m^2\omega_0^2}. \end{aligned} \tag{44}$$

For a sphere ($n^{(x)} = 1/3$),

$$\begin{aligned} \omega_{sca}^2 &\approx \omega_0^2 - \frac{(2\varepsilon_\infty-5\varepsilon_m)\gamma^2}{6\varepsilon_m} \\ &-\frac{(\varepsilon_\infty-\varepsilon_m)(3\varepsilon_m-2\varepsilon_\infty)\gamma^4}{18\varepsilon_m^2\omega_0^2}-\frac{(\varepsilon_\infty-\varepsilon_m)\gamma^4}{18\varepsilon_m\omega_0^2}. \end{aligned} \tag{45}$$

For the scattering cross section, the resonance frequency obtained by Eq. (42) is analytical but cumbersome, so we give the approximate result as shown in Eq. (44), under the condition $\omega_0^2 \gg \gamma^2$. Under this condition the third and fourth terms in Eq. (44) are relatively small, so ω_{sca} is close to ω_0 but less than it for the usual high-frequency dielectric functions of materials, the effect of which can be found in many studies [32, 33].

3.2. Dynamic Depolarization Factor and Radiation Term

In the quasistatic approximation, size effects are not included. If considering size effects, the modified long-wavelength approximation [25, 26] can be used. The depolarization field E_p is

$$E_p = -n^{(x)} P/\varepsilon_0. \tag{46}$$

If considering the dielectric retarded polarization and radiation damping, the dynamic depolarization factor and radiation damping term can be introduced. Further, the depolarization field E_p can be written as follows:

$$E_p = -n_{\text{eff}}^{(x)} \frac{P}{\varepsilon_0} = -(n^{(x)} - b_1 k^2 - i b_2 k^3) \frac{P}{\varepsilon_0}, \tag{47}$$

where $n_{\text{eff}}^{(x)}$ is the effective depolarization factor with the inclusion of the finite-wavelength correction [26], k is the wave vector, and b_1 and b_2 are coefficients. $b_1 k^2$ is associated with the dielectric retarded polarization, and $b_2 k^3$ is associated with the radiation damping [25]. In addition, for oblate and prolate ellipsoids, the depolarization factors and the dynamic depolarization factors and radiation terms can be found in the [26, 34, 35].

The results under the modified long-wave approximation can be obtained by replacing $n^{(x)}$ with $n_{\text{eff}}^{(x)}$ [26]. The electric field in the ellipsoid is

$$\begin{aligned} E_{\text{total}} &= \frac{\sigma_{\text{total}}}{\sigma_f} E_f \\ &= \frac{\varepsilon_\infty - \varepsilon_m}{\varepsilon_m + (\varepsilon_\infty - \varepsilon_m) n_{\text{eff}}^{(x)}} E_0 n_{\text{eff}}^{(x)} \\ &\quad + \frac{\rho d / \varepsilon_0}{\varepsilon_m + (\varepsilon_\infty - \varepsilon_m) n_{\text{eff}}^{(x)}} n_{\text{eff}}^{(x)}. \end{aligned} \tag{48}$$

Thus, the equation of motion is

$$\begin{aligned} &m\ddot{d} + m\gamma'\dot{d} + m\omega_0^2 d = \\ &\frac{\sqrt{[\varepsilon_m(\varepsilon_\infty - \varepsilon_m)(n^{(x)} - b_1 k^2) + \varepsilon_m^2]^2 + [b_2 k^3 \varepsilon_m (\varepsilon_\infty - \varepsilon_m)]^2}}{[(\varepsilon_\infty - \varepsilon_m)(n^{(x)} - b_1 k^2) + \varepsilon_m]^2 + [b_2 k^3 (\varepsilon_\infty - \varepsilon_m)]^2} \\ &\cdot eE_0 \exp(i\phi), \end{aligned} \tag{49}$$

where

$$\exp(i\phi) = \frac{\varepsilon_m(\varepsilon_\infty - \varepsilon_m)(n^{(x)} - b_1 k^2) + \varepsilon_m^2 + i b_2 k^3 \varepsilon_m (\varepsilon_\infty - \varepsilon_m)}{\sqrt{[\varepsilon_m(\varepsilon_\infty - \varepsilon_m)(n^{(x)} - b_1 k^2) + \varepsilon_m^2]^2 + [b_2 k^3 \varepsilon_m (\varepsilon_\infty - \varepsilon_m)]^2}}. \tag{50}$$

The intrinsic frequency ω_0 is

$$\omega_0^2 = \frac{(\varepsilon_\infty - \varepsilon_m)(n^{(x)} - b_1 k^2)^2 + \varepsilon_m (n^{(x)} - b_1 k^2) + b_2^3 k^6 (\varepsilon_\infty - \varepsilon_m)}{[\varepsilon_m + (\varepsilon_\infty - \varepsilon_m)(n^{(x)} - b_1 k^2)]^2 + [(\varepsilon_\infty - \varepsilon_m) b_2 k^3]^2} \omega_p^2, \tag{51}$$

where the intrinsic frequency or the restoring force is affected by the high-frequency dielectric function of the particle ε_∞, the dielectric function of the medium ε_m, the plasma frequency ω_p, and the dynamic depolarization factor and the radiation damping term.

The damping term is

$$\gamma' = \gamma + \frac{1}{\omega} \frac{b_2 k^3 \varepsilon_m \omega_p^2}{[\varepsilon_m + (\varepsilon_\infty - \varepsilon_m)(n^x - b_1 k^2)]^2 + [(\varepsilon_\infty - \varepsilon_m) b_2 k^3]^2}, \tag{52}$$

where the first term arises from the damping of the collective motion of free charges, and the second term arises from the radiation damping of the electric dipole formed by the free and bound charges. The driving force has a phase delay compared to the force of the external electric field E_0, as shown in Eq. (50), which arises from the radiation damping of the dipoles.

3.3. Discussion

The displacement of the harmonic oscillator is that between the positive and negative free charges, and its magnitude is influenced by the high-frequency dielectric function of the particle, the dielectric function of the medium, and the dynamic depolarization factor and the radiation damping term. In our model the displacement is related to free charges, as shown in Fig. 1. The maximum displacement corresponds to the maximum accumulation of surface free charges.

The actual driving force is not equal to the force of the incident light field. It is affected by the dielectric function of the surrounding medium, the dielectric function of the dielectric background, and the shape factor $n^{(x)}$. Considering also the dynamic depolarization factor and radiation term, the actual driving force is also affected by them. Furthermore, when the radiation term is considered, a phase delay exists between the actual driving force and the external field.

It is interesting that the peak position of the extinction cross section is simply the intrinsic frequency ω_0 of the material. The resonance frequency of the scattering cross section is slightly smaller than that of the extinction cross section. The resonance frequency of the harmonic oscillator equation [see Eq. (32)] is lower than ω_0, which is attributed to the peak position for the near field [23]. In the oscillator model, this resonant frequency generates the maximum displacement of the oscillator.

As we know, when the frequency tends to zero, the imaginary part of the dielectric function of the Drude model as shown in Eq. (1) will tend to infinity, which is the deficiency of the Drude model. The Drude model is not used in our harmonic oscillator model. In our model there is no

conflict, because free charges always accumulate on the surfaces and generate the dipole moment, even when the frequency tends to zero. Our model avoids the limitation of the dielectric function of the metal. The two models are based on the same physical picture, so they are equivalent, and the same extinction and scattering cross section results can be obtained. In addition, the damping γ for both models is the same, due to the same collective motion of free charges.

The forced damped harmonic oscillator model, which is a very intuitive physical picture for the LSPR, can be used to understand the physical source of the LSPR caused by the collective motion of electrons in metal. Based on this harmonic oscillator model, the LSPR is no longer limited to metals. Semiconductors with free charges can also exhibit the LSPR, and the resonance can be modulated by the density of the doping [3, 5–9]. In recent years a few carriers in a small nanoparticle, even four carriers in a ZnO nanoparticle [36], have been found to sustain the surface plasmon from the collective motion of those carriers [9]. In understanding these phenomena, the picture of carriers oscillating under the driving field is more intuitive than that of the collective motion of the carriers, which is attributed to the dielectric function of the nanoparticle. In the harmonic oscillator model, the density of the carriers determines the magnitude of the scattering and extinction, and the resonance frequencies. Our model provides a basic theoretical understanding of plasmonic phenomena.

IV. CONCLUSIONS

We have derived analytical expressions for the LSPR, based on the collective motion of free charges by the forced damped oscillator model. The extinction cross section and scattering cross section and their resonance frequencies were derived under the harmonic oscillator model, the results of which are consistent with those of the Drude model. This means those two models are equivalent, due to the same collective motion picture, and their parameters are the same, such as γ. After we further introduce size effects, the expression can be extended by including the effective depolarization factor in the harmonic oscillator model. The restoring force and the driving force will be modified by the high-frequency dielectric function of the dielectric background, the dielectric function of the medium, the depolarization factor of the ellipsoid, the dynamic depolarization term, and the radiation term. The driving force has a phase shift from the external field, due to the radiation term. According to our model, the dipole plasmon mode arises from the collective motion of free charges, modulated by the bound charges and radiation of the dipole moment formed by free charges and the bound charges. This theoretical model describes an intuitive picture of the LSPR that can be applied to particles containing free charges in metals or semiconductors.

FUNDING

Central Universities (FRF-BR-19-002B); Scientific Research Foundation for the Returned Overseas Chinese Scholars (48th); Beijing Higher Education Young Elite Teacher Project (No YETP0391).

DISCLOSURES

The authors declare no conflict of interest.

DATA AVAILABILITY

No data were generated or analyzed in the current study.

REFERENCES

1. X. Zhang and Q. Li, "Forced damped harmonic oscillator model of the dipole mode of localized surface plasmon resonance," Plasmonics **16**, 1525–1536 (2021).
2. J. Katyal and R. K. Soni, "Field enhancement around al nanostructures in the DUV–visible region," Plasmonics **10**, 1729–1740 (2015).
3. A. Agrawal, S. H. Cho, O. Zandi, S. Ghosh, R.W. Johns, and D. J. Milliron, "Localized surface plasmon resonance in semiconductor nanocrystals," Chem. Rev. **118**, 3121–3207 (2018).
4. T. A. Tabish, P. Dey, S. Mosca, M. Salimi, F. Palombo, P. Matousek, and N. Stone, "Smart gold nanostructures for light mediated cancer theranostics: Combining optical diagnostics with photothermal therapy," Adv. Sci. **7**, 1903441 (2020).
5. J. Son, D. Choi, M. Park, J. Kim, and K. S. Jeong, "Transformation of colloidal quantum dot: from intraband transition to localized surface plasmon resonance," Nano Lett. **20**, 4985–4992 (2020).
6. J. S. Niezgoda and S. J. Rosenthal, "Synthetic strategies for semiconductor nanocrystals expressing localized surface plasmon resonance," Chem. Phys. Chem. **17**, 645–653 (2015).
7. G. V. Naik, V. M. Shalaev, and A. Boltasseva, "Alternative plasmonic materials: Beyond gold and silver," Adv. Mater. **25**, 3264–3294 (2013).
8. J. Jung and T. G. Pedersen, "Analysis of plasmonic properties of heavily doped semiconductors using full band structure calculations," J. Appl. Phys. **113**, 114904 (2013).
9. P. K. Jain, "Plasmon-in-a-box: On the physical nature of few-carrier plasmon resonances," J. Phys. Chem. Lett. **5**, 3112–3119 (2014).
10. Y. Li, H. Guo, Z. Yin, K. Lyle, and L. Tian, "Metal-organic frameworks for preserving the functionality of plasmonic nanosensors," ACS Appl. Mater. Interf. **13**, 5564–5573 (2021).
11. X. Han, K. Liu, and C. Sun, "Plasmonics for biosensing," Materials **12**, 1411 (2019).
12. M. Kraft, Y. Luo, S. A. Maier, and J. B. Pendry, "Designing plasmonic gratings with transformation optics," Phys. Rev. X. **5**, 031029 (2015).
13. R.-H. Fan, L.-H. Zhu, R.-W. Peng, X.-R. Huang, D.-X. Qi, X.-P. Ren, Q. Hu, and M. Wang, "Broadband antireflection and

light-trapping enhancement of plasmonic solar cells," Phys. Rev. B. **87**, 195444 (2013).
14. V. Awasthi, R. Goel, S. Agarwal, P. Rai, and S. K. Dubey, "Optical nanoantenna for beamed and surface-enhanced Raman spectroscopy," J. Raman Spectrosc. **51**, 2121–2145 (2020).
15. P. K. Jain, X. Huang, I. H. El-Sayed, and M. A. El-Sayed, "Noble metals on the nanoscale: Optical and photothermal properties and some applications in imaging, sensing, biology, and medicine," Acc. Chem. Res. **41**, 1578–1586 (2008).
16. O. A. Balitskii, "Recent energy targeted applications of LSPR semiconductor nanocrystals: A mini-review," Mater. Today Energy **20**, 100629 (2020).
17. S. Lal, S. E. Clare, and N. J. Halas, "Nanoshell-enabled photothermal cancer therapy: Impending clinical impact," Acc. Chem. Res. **41**, 1842–1851 (2008).
18. C. F. Bohren and D. R. Huffman, *Absorption and Scattering of Light by Small Particles* (Wiley- VCH, Germany, 1983).
19. C. Ciracì, J. B. Pendry, and D. R. Smith, "Hydrodynamic model for plasmonics: A macroscopic approach to a microscopic problem," Chem. Phys. Chem. **14**, 1109–1116 (2013).
20. E. Prodan, C. Radloff, N. J. Halas, and P. Nordlander, "A hybridization model for the plasmon response of complex nanostructures," Science **302**, 419–422 (2003).
21. Y. Li, K. Zhao, H. Sobhani, K. Bao, and P. Nordlander, "Geometric dependence of the line width of localized surface plasmon resonances," J. Phys. Chem. Lett. **4**, 1352–1357 (2013).
22. W. Rechberger, A. Hohenau, A. Leitner, J. R. Krenn, B. Lamprecht, and F. R. Aussenegg, "Optical properties of two interacting gold nanoparticles," Opt. Commun. **220**, 137–141 (2003).
23. J. Zuloaga and P. Nordlander, "On the energy shift between near-field and far-field peak intensities in localized plasmon systems," Nano Lett. **11**, 1280–1283 (2011).
24. J. Zhu and X.-C. Deng, "Improve the refractive index sensitivity of gold nanotube by reducing the restoring force of localized surface plasmon resonance," Sens. Actuator B: Chem. **155**, 843–847 (2011).
25. M. Meier and A. Wokaun, "Enhanced fields on large metal particles: Dynamic depolarization," Opt. Lett. **8**, 581–583 (1983).
26. M. Januar, B. Liu, J.-C. Cheng, K. Hatanaka, H. Misawa, H.-H. Hsiao, and K.-C. Liu, "Role of depolarization factors in the evolution of a dipolar plasmonic spectral line in the far- and near-field regimes," J. Phys. Chem. C **124**, 3250–3259 (2020).
27. P. Mulvaney, "Surface plasmon spectroscopy of nanosized metal particles," Langmuir **12**, 788–800 (1996).
28. M. Born and K. Huang, *Dynamic theory of Crystal lattices* (Oxford University Press, UK, 1954).
29. F. Tam, A. L. Chen, J. Kundu, W. Hui, and N. J. Halas, "Mesoscopic nanoshells: Geometry-dependent plasmon resonances beyond the quasistatic limit," J. Chem. Phys. **127**, 204703 (2007).
30. J. A. Stratton, *Electromagnetic theory* (John Wiley & Sons, NY, USA, 2007).
31. L. D. Landau and E. M. Lifshitz, *Electrodynamics of continuous media* (Pergamon Press, UK, 1960), Vol. 8.
32. S. Y. Wu, W. M. Chang, H. Y. Tseng, C. K. Lee, T. T. Chi, J. Y. Wang, Y. W. Kiang, and C. C. Yang, "Geometry for maximizing localized surface plasmon resonance of Au nanorings with random orientations," Plasmonics **6**, 547–555 (2011).
33. S.-E. Yang, P. Liu, Y.-J. Zhang, Q. N. Guo, and Y.-S. Chen, "Effects of silver nanoparticles size and shape on light scattering," Optik **127**, 5722–5728 (2016).
34. M. R. A. Majić, B. Auguié, and E. C. L. Ru, "Comparison of dynamic corrections to the quasistatic polarizability and optical properties of small spheroidal particles," J. Chem. Phys. **156**, 104110 (2022).
35. A. Moroz, "Depolarization field of spheroidal particles," J. Opt. Soc. Am. B **26**, 517–527 (2009).
36. J. A. Faucheaux and P. K. Jain, "Plasmons in photocharged ZnO nanocrystals reveal nature of charge dynamics," J. Phys. Chem. Lett. **4**, 3024–3030 (2013).